A Multitasking Electric Power Dispatch Approach With Multi-Objective Multifactorial Optimization Algorithm

JUNWEI LIU [1,2], **PEILING LI**[1], **GUIBIN WANG** [1], **(Member, IEEE),**
YONGXING ZHA[1], **JIANCHUN PENG**[1], **(Senior Member, IEEE), AND GANG XU**[3]

[1]College of Mechatronics and Control Engineering, Shenzhen University, Shenzhen 518060, China
[2]Key Laboratory of Optoelectronic Devices and Systems of Ministry of Education and Guangdong Province, College of Optoelectronic Engineering, Shenzhen University, Shenzhen 518060, China
[3]College of Urban Transportation and Logistics, Shenzhen Technology University, Shenzhen 518118, China

Corresponding author: Guibin Wang (wanggb@szu.edu.cn)

ABSTRACT Electric power dispatch issue mainly consists of two optimization tasks: active and reactive power dispatches, each of which is a non-linear multi-objective optimization problem with a series of constraints. Traditional evolutionary algorithms are focused on single-task optimization for active or reactive power dispatch and they are not able to deal with several (single- or multi-objective) optimization tasks simultaneously. In this paper, to solve this problem, a multitasking electric power dispatch approach is proposed by introducing the multi-objective multifactorial optimization (MO-MFO) algorithm and integrating it with the characteristics of power system. The approach exhibits the great potential to be developed as a cloud-computing solver or platform for future large-scale smart grid applications involving different market entities because of its implicit parallel computation mechanism. The multitasking approach is thoroughly tested and benchmarked with IEEE-30-bus and IEEE-118-bus standard systems and exhibits generally better performances as compared to previously proposed Pareto heuristic approaches for electric power dispatch.

INDEX TERMS Electric power dispatch, multifactorial, multitasking, optimization.

I. INTRODUCTION

Active and reactive power dispatches are two significant tasks for optimal and safety operations of modern power systems. As the increasing significance of energy saving and emission reduction draws more and more attention from the industrial community, the conventional single-objective electric power dispatch techniques which simply pursue the minimum cost, minimum emission, or minimum voltage variation cannot fulfill the requirements of the modern energy management system and the smart power grid. In recent years, the electric power dispatch problem considered as a multi-objective optimization issue which simultaneously tries to find multiple incommensurable and contradictory targets under a set of safety and operation constraints has received much attention. Optimal active power dispatch (APD) requires minimizing cost, emission, and transmission loss and reactive power dispatch (RPD) requires minimizing voltage variation and

The associate editor coordinating the review of this manuscript and approving it for publication was Bin Zhou [ID].

transmission loss and maximizing voltage stability. For a single dispatch task, because of the mutual contradiction of those objectives, the target is to find its Pareto-optimal fronts.

For the multi-objective problem in electric power dispatch, there exist two categories of optimization techniques: the first is the traditional linearization math method while another is the Pareto-based heuristic technique. For high dimensional multi-objective complex non-linear problems, the Pareto-based heuristic approach would have advantages and it includes Niched Pareto genetic algorithm (NPGA) [1], non-dominated sorting genetic algorithm (NSGA) [1], NSGA-II [2], strength Pareto evolutionary algorithm (SPEA) [3], multiple group search optimization algorithm (MGSO) [4], [5], etc.

The aforementioned optimization approaches are limited to solve one multi-objective task at a time. In other words, for one computing engine, they are not able to deal with more than one optimization tasks simultaneously; instead, those tasks will be processed serially. A modern power

grid, as a complex system involving economic/environmental dispatch, electric transportation planning, communication network maintenance, electricity market transaction, fault diagnosis, and condition estimation, etc., generally requires many computation engines and processors to handle such enormous and complicated task load in real time. To reduce the hardware requirements of computation engines and increase the computation efficiencies, a cloud computing platform that is capable of handling different kinds of tasks simultaneously (parallel computation) would be an advantageous alternative. Recently, an evolutionary multitasking technique that harnesses the implicit parallelism of a population-based search to cope with multiple optimization tasks simultaneously with a single population was proposed for cloud-based applications [6] – [8]. It considers each optimization task as an additional factor affecting the total evolutionary process and therefore is named as multi-objective multifactorial optimization (MO-MFO) algorithm. Currently, it is designed and explored as a multitasking solver, especially for multiple optimization problems, while it exhibits great potential to be developed as a multitasking general problem-solving engine and applied in the cloud computing platform for the aforesaid modern power grid with many complex problems.

In this paper, the multi-objective multifactorial optimization (MO-MFO) algorithm is creatively applied in the electric power dispatch problems. And a multitasking electric power dispatch approach is further developed and proposed by integrating the MO-MFO algorithm with the characteristics of power system models in order to optimize both active and reactive power dispatch tasks concurrently, as well as reduce the execution time, and improve the performances. The analysis and design of the approach have been thoroughly verified and benchmarked with IEEE-30-bus and IEEE-118-bus standard systems. As compared to the other evolutionary techniques for electric power dispatch, including NSGA-II, MGSO, and MOEA/D methods, the proposed approach exhibits much better in terms of the evaluation metrics, solution qualities, and the computation efficiency.

II. MULTI-OBJECTIVE MULTIFACTORIAL OPTIMIZATION
A. FRAMEWORK AND PRINCIPLE OF THE ALGORITHM
The essential target of MO-MFO is to solve multiple multi-objective optimization problems simultaneously by mining their potential implicit parallelism, and furtherly to make those multi-objective optimization problems under different environments with shorter execution time and better optimization performances. The implicit parallel processing principle is achieved using the unified search space which contains the design spaces of several different tasks [6] – [8]. The optimal chromosome is searched in the unified search space and it could be decoded into the corresponding solution variables associated with the tasks. Therefore, several different tasks are optimized with only one search solver. In the following, the details will be explained with the assistance of Fig. 1.
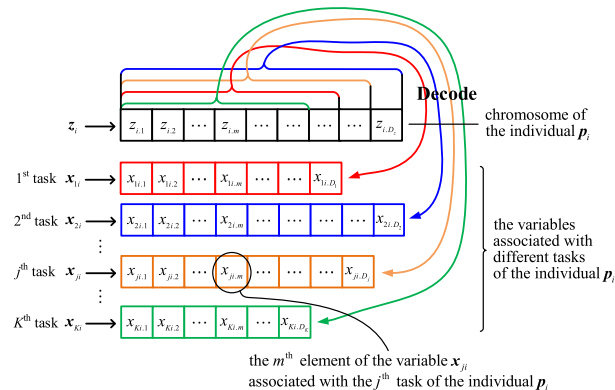

FIGURE 1. The chromosome of the ith individual and its relations with the variables of different tasks.

For multiple optimization tasks, some of them may be complimentary with some other tasks, and genetic material and useful information can be transferred across those tasks, which may result in speeding up the total optimization process. It has been studied and verified that useful knowledge transferred across different but related tasks, such as CVRP and CARP problems [9], will help improve the performances of evolutionary optimization.

Before illustrating the principle of the MO-MFO algorithm, we firstly make the essential definitions and notations for the related variables and parameters. In the theoretical scenario of multi-task, there are K different multi-objective optimization tasks, that are assumed to be the minimization problems without loss of generality. For the jth task T_j, the objective function $\boldsymbol{F}_j$ is defined as:

$$\boldsymbol{F}_j : \boldsymbol{X}_j \rightarrow \boldsymbol{R}^{M_j}, \tag{1}$$

where $\boldsymbol{X}_j$ is the design space (or called as the decision variable space) of the jth task, $\boldsymbol{R}^{Mj}$ is the objective function space of the jth task with the dimension of M_j. The dimension of the design space $\boldsymbol{X}_j$ is noted as D_j. The objective function value $\boldsymbol{y}_j$ can be expressed as:

$$\boldsymbol{y}_j = \left(y_{j.1}, y_{j.2}, \ldots, y_{j.M_j} \right), \tag{2}$$

and $\boldsymbol{x}_j$ is the design variable of the jth task:

$$\boldsymbol{x}_j = \left(x_{j.1}, x_{j.2}, \ldots, x_{j.D_j} \right), \tag{3}$$

Therefore, the objective function $\boldsymbol{F}_j$ maps design variables $\boldsymbol{x}_j$ to vectors $\boldsymbol{y}_j$, which is also expressed as:

$$\boldsymbol{y}_j = \boldsymbol{F}_j \left(\boldsymbol{x}_j \right) = \left(f_{j1} \left(\boldsymbol{x}_j \right), f_{j2} \left(\boldsymbol{x}_j \right), \ldots, f_{jM_j} \left(\boldsymbol{x}_j \right) \right). \tag{4}$$

For a single task T_{j}, the Pareto optimal set $\boldsymbol{PS}_j$ is defined as:

$$\boldsymbol{PS}_j = \left\{ \boldsymbol{x}_j \in \boldsymbol{X}_j | \neg \exists \boldsymbol{x}'_j \in \boldsymbol{X}_j : \boldsymbol{F}_j \left(\boldsymbol{x}'_j \right) \succeq \boldsymbol{F}_j \left(\boldsymbol{x}_j \right) \right\}, \tag{5}$$

And the Pareto front $\boldsymbol{PF}_j$ is defined as:

$$\boldsymbol{PF}_j = \left\{ \boldsymbol{y}_j = \boldsymbol{F}_j \left(\boldsymbol{x}_j \right) = \left(f_{j1} \left(\boldsymbol{x}_j \right), \ldots, f_{jM_j} \left(\boldsymbol{x}_j \right) \right) | \boldsymbol{x}_j \in \boldsymbol{PS}_j \right\}. \tag{6}$$

For the multitasking environment, the target is to find the Pareto sets of all the tasks $\boldsymbol{PS}_1, \boldsymbol{PS}_2, \ldots, \boldsymbol{PS}_K$.

However, for the proposed MO-MFO algorithm, the target is to find one optimal individual that consists of the information of all the tasks' optimal solution. In other words, such an optimal individual can be translated into the specific solution of any of the optimization tasks. In the evolutionary process of the proposed algorithm, there are a number of individuals existing in the population $\boldsymbol{P}$, and each individual is defined as $\boldsymbol{p}_i$ and

$$i \in \{1, 2, \ldots, N\}, \tag{7}$$

where N is the total number of individuals. Next, a unified search space $\boldsymbol{Z}$ is defined, which encompasses the design spaces of all the tasks $X_1, X_2, \ldots, X_K$. Every individual $\boldsymbol{p}_i$ is encoded, and its chromosome z_i belongs to the unified search space $\boldsymbol{Z}$. The dimension of $\boldsymbol{Z}$ is selected as the maximum of the design spaces' dimensions:

$$D_Z = \max \{D_1, D_2, \ldots, D_K\}. \tag{8}$$

For the individual $\boldsymbol{p}_i$, as shown in Fig. 1, its chromosome z_i contains the information of K variables $(\boldsymbol{x}_{1i}, \boldsymbol{x}_{2i}, \ldots, \boldsymbol{x}_{Ki})$ associated with K tasks. Each element of the variables can be decoded from the corresponding element of the chromosome of $\boldsymbol{p}_i$. Here in the paper, the element of the chromosome is also called as random-key, and the variables of different tasks are called as solution representations. For the continuous case, note the mth random-key of z_i as $z_{i.m}$ and it is assumed to be limited in the range of $[0, 1]$. For the specific j^{th} task, the mth element of $\boldsymbol{x}_{ji}$ is defined as $x_{ji.m}$ and box-constrained as $[L_{j.m}, U_{j.m}]$, and one sample of the decoding method is shown as:

$$x_{ji.m} = L_{j.m} + z_{i.m} \cdot (U_{j.m} - L_{j.m}). \tag{9}$$

In addition to the aforementioned decoding method, different representations may apply to other decoding methods, such as binary decoding, sequence-based decoding, etc., according to the specific requirements of different tasks. Following, there are three essential definitions (factorial rank, skill factor, and scalar fitness) needed to be illustrated in detail. The factorial rank r_j^i of $\boldsymbol{p}_i$ for task T_j is defined as the rank of $\boldsymbol{p}_i$'s effectiveness regarding task T_j in the list of $\boldsymbol{P}$'s members. The skill factor τ_i of $\boldsymbol{p}_i$ is defined as the task index number of the one task, with which $\boldsymbol{p}_i$ is associated. If $\boldsymbol{p}_i$ is evaluated for all tasks, τ_i will be the task index number of the one task, to which $\boldsymbol{p}_i$ is the most effective:

$$\tau_i = \operatorname*{arg\,min}_{j \in \{1,2,\ldots,K\}} \{r_j^i\}, \tag{10}$$

The scalar fitness φ_i of $\boldsymbol{p}_i$ in the multitasking environment is based on $\boldsymbol{p}_i$'s best rank amongst all tasks, defined as:

$$\varphi_i = 1 \Big/ r_{\tau_i}^i = 1 \Big/ \min \{r_1^i, r_2^i, \ldots, r_K^i\}. \tag{11}$$

The sorting of the factorial rank r_j^i of $\boldsymbol{p}_i$ for task T_j is based on the non-dominated front (NF) [10] and crowding distance (CD) [11] of task T_j's objective functions' values with the specific solution representation $\boldsymbol{x}_{ji}$ decoded from the chromosome z_i of $\boldsymbol{p}_i$. Note the aforementioned NF and
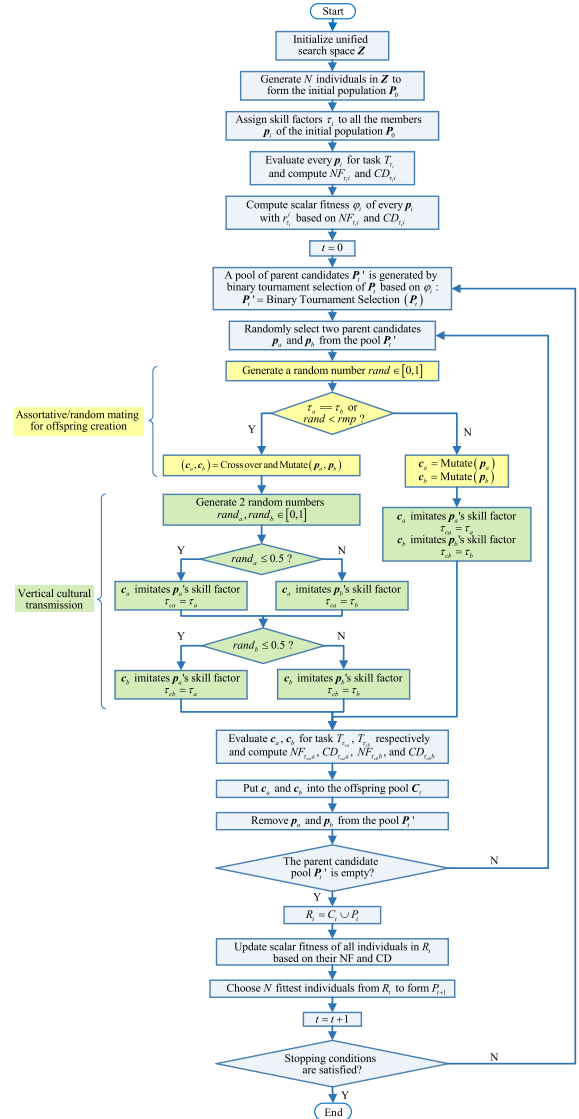

FIGURE 2. Detailed flow chart of the MO-MFO algorithm.

CD as NF_{ji} and CD_{ji}, respectively. For example, when we compare $\boldsymbol{p}_1$ and $\boldsymbol{p}_2$'s factorial ranks (r_j^1 and r_j^2) for task T_j, $\boldsymbol{p}_1$ is considered to be preferred over $\boldsymbol{p}_2$, meaning $\boldsymbol{p}_1$ has a better rank than $\boldsymbol{p}_2$ ($r_j^1 < r_j^2$), when any one of the following conditions is satisfied:

$$NF_{j1} < NF_{j2}, \tag{12}$$

$$NF_{j1} = NF_{j2} \quad \text{and} \quad CD_{j1} > CD_{j2}. \tag{13}$$

With the definitions of factorial rank, skill factor, and scalar fitness, the MO-MFO algorithm is illustrated with the assistance of the flow chart in Fig. 2. Firstly, a unified search space $\boldsymbol{Z}$ is initialized, and N individuals are generated from the space to form the initial population $\boldsymbol{P}_0$. Next, all the members $\boldsymbol{p}_i$ of the population $\boldsymbol{P}_0$ are randomly assigned their skill factors τ_i and then evaluated for task $T_{\tau i}$ with the decoding procedure and objective functions. The assignment needs to guarantee that each task is uniformly associated. Further, the scalar fitness φ_i of every $\boldsymbol{p}_i$ is calculated based

on the NF and CD. To generate offspring, a pool of parent candidates noted as $P' t$, is generated from the current population using binary tournament selection method. After that are the assortative or random mating for offspring creation, and the skill factor assignment for new offspring, which can be comprehended as vertical cultural transmission. Then the new offspring individuals are evaluated for the task associated with their skill factors and put into the offspring pool C_t. The processes of offspring creation and skill factor assignment are repeated several times until the parent candidates pool $P' t$ is empty. When the offspring pool C_t is ready, a temporary candidate pool R_t consisting of C_t and P_t is formed with all the individuals' scalar fitness updated. Finally, N fittest individuals are chosen from R_t to form a new population P_{t+1}. Such evolving processes will be repeated multiple times until stop conditions are satisfied.

Offspring individuals are created from the parent candidates pool by assortative or random mating methods. If two parent individuals, which are randomly selected from the parent candidates pool, are with the same skill factors, they will undergo both crossover and mutate processes to generate two offspring individuals, as explained by the phenomenon of assortative mating. For the condition with different skill factors, they still have a probability (random mating probability, noted as *rmp*) to undergo crossover and mutate processes, which is understood as the natural phenomenon of random mating. For other conditions, they simply undergo mutation to generate two mutant offspring individuals separately. The principle of assortative mating indicates that in nature individuals prefers to mate with those with identical cultural attribute. However, individuals with different cultural attributes still have a probability to mate with each other, which is explained as the principle of random mating. The random mating probability is estimated roughly according to the correlation degree of the involved tasks. A higher correlation degree leads to a larger probability. The detailed steps of offspring creation are presented in Fig. 2.

Vertical cultural transmission is a natural phenomenon that illustrates the offspring imitate the cultural features of their parents according to cultural and biological inheritance theory [12]. The natural phenomenon is applied in the MO-MFO algorithm where the offspring individuals imitate any one of the skill factors of their parents randomly. For the offspring individual generated simply from the only mutation, it imitates the skill factor of its single parent simply.

The implicit information transfer between different tasks in the MO-MFO algorithm is achieved by the random mating probability of two parent candidates with distinct skill factors and the offspring's random selection of skill factor from its parents. Such stochastic processes guarantee the inter-task knowledge transmission for the multitasking environment.

B. POTENTIAL FOR FUTURE SMART GRID APPLICATIONS

In addition to optimization problems, the MO-MFO algorithm exhibits large potentials of being developed as a complex multi-objective multitasking solver, and furthermore,
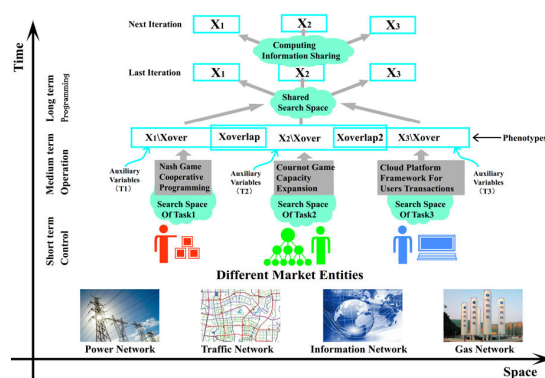

FIGURE 3. Example of future smart grid application with multi-objective multitasking cloud-computing platform.

a cloud-computing platform involving different market entities including power network, traffic network, information network, gas network, and so on. For example, the complex operations of a multi-energy system including electricity, heating, and natural gas networks [13] can be furtherly optimized with the aforementioned platform. All the tasks of those networks can be computed and solved simultaneously with a shared search space with reduced space requirements and improved computing efficiencies. Fig. 3 shows an example of multi-objective multitasking cloud-computing platform for future smart grid applications with several representative tasks, such as Nash game problem for cooperative planning, Cournot game problem for capacity expansion, and cloud framework for users' transactions, whose phenotypes may have part of overlaps with each other and enable useful information sharing and transmission and hence the computations are accelerated. Originally there are separate search spaces regarding those tasks respectively. In the platform, the separate search spaces are integrated into one shared search space. In the shared search space, each task's computing information is shared with others. From the last iteration to the next iteration, the population is updated with newly generated and better offspring individuals within the shared search space. Further, for the sake of using a shared search space instead of three separate search spaces, space and memory resources are reduced significantly. The example in Fig. 3 is simply introduced to show the algorithm's great development potentials for future smart grid applications and will not be discussed in detail in this paper. Instead, the optimization problem of active and reactive electric power dispatches is discussed in the following in order to validate the algorithm's applicability and advantages. The tasks of active and reactive electric power dispatches are related because they rely on the same power system model, and they have one common objective – transmission loss minimization. Hence, the algorithm is appropriate.

III. MODELS OF ACTIVE AND REACTIVE POWER DISPATCHES

Active and reactive power dispatches are considered as two optimization tasks with respective objectives and constraints.

A. ACTIVE POWER DISPATCH (APD)

1) OBJECTIVES OF APD

The optimization objectives of active power dispatch consist of economic objective, emission objective, and transmission loss objective.

a: ECONOMIC OBJECTIVE

Minimization of total generation (fuel) cost is defined as the economic objective of APD, with the corresponding objective function [14] described as:

$$F(P_G) = \sum_{i=1}^{N_G} \left\{ a_i P_{Gi}^2 + b_i P_{Gi} + c_i + |d_i \sin[e_i (P_{Gi.min}\right.$$
$$\left. -P_{Gi})]| \right\}. \quad (14)$$

where F is total fuel cost in (\$/h); P_{Gi} and $P_{Gi.min}$ are the actual output power and minimum output power of the ith generator; $(a_i, b_i, c_i, d_i, e_i)$ are the cost coefficients of the ith generator; and N_G is the total count of generators.

b: EMISSION OBJECTIVE

Minimization of total fossil fuel pollutants (emission) during generation process is defined as the emission objective of APD, with the corresponding objective function [15] described as:

$$E(P_G) = \sum_{i=1}^{N_G} 10^{-2} \left[\alpha_i P_{Gi}^2 + \beta_i P_{Gi} + \gamma_i + \zeta_i \exp(\lambda_i P_{Gi}) \right]. \quad (15)$$

where E is the total emission in (ton/h) and $(\alpha_i, \beta_i, \gamma_i, \zeta_i, \lambda_i)$ are the emission coefficients of the ith generator.

c: TRANSMISSION LOSS OBJECTIVE

Minimization of power losses in transmission lines is defined as the transmission loss objective of APD. The total transmission losses [1] can be calculated with the Newton-Raphson method and expressed as:

$$P_{Loss} = \sum_{z=1}^{N_L} g_z \left[V_x^2 + V_y^2 - 2V_x V_y \cos(\delta_x - \delta_y) \right]. \quad (16)$$

where $x \in \{1, 2, \ldots, N_B\}$ and N_L is the number of transmission lines; g_z is the conductance of the zth line connecting the xth and the yth buses; V_x, δ_x are the voltage magnitudes and angles of the xth bus; and V_y, δ_y are the voltage magnitudes and angles of the yth bus. Voltage magnitudes and angles at all buses can be obtained by load-flow calculation with Newton-Raphson method:

$$P_{gx} - P_{lx} - V_x \sum_{y=1}^{N_B} V_y \left[G_{xy} \cos(\delta_x - \delta_y) \right.$$
$$\left. + B_{xy} \sin(\delta_x - \delta_y) \right] = 0, \quad (17)$$

$$Q_{gx} - Q_{lx} - V_x \sum_{y=1}^{N_B} V_y \left[G_{xy} \sin(\delta_x - \delta_y) \right.$$
$$\left. - B_{xy} \cos(\delta_x - \delta_y) \right] = 0. \quad (18)$$

where N_B is the number of buses; P_{gx} and Q_{gx} are the generated active and reactive power at the xth bus respectively; P_{lx} and Q_{lx} are the load active and reactive power at the xth bus respectively; G_{xy} and B_{xy} are the transfer conductance and susceptance between the xth and y^{th} buses respectively.

2) CONSTRAINTS OF APD

During the operation progress of power system, there are several practical operations, and safety requirements need to be satisfied, which are modeled as the constraints of the optimization task.

a: POWER BALANCE CONSTRAINT

The total generated power of generators should be equal to the load demand power and the total transmission losses, which can be expressed as:

$$\sum_{i=1}^{N_G} P_{Gi} - \sum_{x=1}^{N_B} P_{lx} - P_{Loss} = 0. \quad (19)$$

b: BUS VOLTAGE CONSTRAINT

The constraint of the voltages at all buses is expressed as:

$$V_{x.\min} \leq V_x \leq V_{x.\max}, \quad x \in \{1, 2, \ldots, N_B\}. \quad (20)$$

where $V_{x.min}$ and $V_{x.max}$ are the allowable lower and upper limits of the xth bus voltage.

c: TRANSMISSION SECURITY CONSTRAINT

The apparent power flowing through every transmission line should be smaller than the corresponding maximum transmission capacity:

$$\max(|S_{xy}|, |S_{yx}|) \leq S_{z.\max}, x, y \in \{1, 2, \ldots, N_B\},$$
$$z \in \{1, 2, \ldots, N_L\}. \quad (21)$$

where S_{xy} is the apparent power flow from the xth bus to the yth bus while S_{yx} is that with the opposite direction; $S_{z.max}$ is the upper limit of the zth transmission line's apparent power.

d: SPINNING RESERVE CONSTRAINT

For the safe and stable operation for the system, the spinning reserve requirement for emergency conditions must be satisfied [17]. The generators with prohibited operating zones are not considered as part of the spinning reserve. The constraint is expressed as:

$$\sum_{i=1}^{N_G} SP_{Gi} \geq SP_R, SP_{Gi} = \begin{cases} 0 & \forall i \in \Omega \\ P_{Gi.\max} - P_{Gi} & \text{others.} \end{cases} \quad (22)$$

where SP_{Gi} is the spinning reserve of the ith generator; SP_R is the spinning reserve requirement; $P_{Gi.max}$ is the maximum output of the ith generator, and Ω is the set of generators with prohibited operating zones.

B. REACTIVE POWER DISPATCH (RPD)

1) OBJECTIVES OF RPD

The optimization objectives of reactive power dispatch are transmission loss objective, voltage profile objective, and voltage stability objective.

a: TRANSMISSION LOSS OBJECTIVE

This objective is to minimize the total power losses in transmission lines during the RPD progress, whose expression is the same as the transmission loss objective of APD.

b: VOLTAGE PROFILE OBJECTIVE

Minimization of the total absolute deviations of voltage magnitudes at the load buses is defined as the voltage profile objective and the sum of the absolute deviations is noted as V_D and described as:

$$V_D = \sum_{k=1}^{N_{LB}} |V_k - V_{k.r}|. \tag{23}$$

where N_{LB} is the number of buses with loads; V_k and $V_{k.r}$ are the actual and rated voltages at the kth load bus, respectively.

c: VOLTAGE STABILITY OBJECTIVE

Voltages at the buses with loads may collapse when contingency conditions happen, and here a global indicator L describing the voltage stability of the system is given as [18]:

$$L = \max_{k \in \{1,2,...,N_{LB}\}} \left| 1 - \frac{\sum_{i=1}^{N_G} F_{ki} \cdot V_{Gi}^c}{V_{Lk}^c} \right|, \tag{24}$$

where V_{Gi}^c and V_{Lk}^c are the voltages at the ith generator bus and the kth load bus in complex form, respectively; F_{ki} is the element of the matrix $\boldsymbol{F}_{LG}$, which is calculated by:

$$\begin{bmatrix} V_L^c \\ I_G^c \end{bmatrix} = [\boldsymbol{H}] \cdot \begin{bmatrix} I_L^c \\ V_G^c \end{bmatrix} = \begin{bmatrix} \boldsymbol{Z}_{LL} & \boldsymbol{F}_{LG} \\ \boldsymbol{K}_{GL} & q\boldsymbol{Y}_{GG} \end{bmatrix} \cdot \begin{bmatrix} I_L^c \\ V_G^c \end{bmatrix}. \tag{25}$$

where V_G^c and I_G^c are voltage and current vectors at generator buses in complex form respectively; V_L^c and I_L^c are voltage and current vectors at load buses in complex form respectively; $\boldsymbol{Z}_{LL}$, $\boldsymbol{F}_{LG}$, $\boldsymbol{K}_{GL}$, and $\boldsymbol{Y}_{GG}$ are sub-matrices of the $\boldsymbol{H}$ matrix which is derived from the nodal admittance matrix with partial inversion.

2) CONSTRAINTS OF RPD

There are six operational and practical constraints of reactive power dispatch, including generation constrains, bus voltage constraint, transmission security constraint, load flow equality constraint, transformer constraint, and VAR source constraint.

a: GENERATION CONSTRAINT

Every generator's active and reactive power outputs are limited in respective ranges:

$$P_{Gi.\min} \leq P_{Gi} \leq P_{Gi.\max}, Q_{Gi.\min} \leq Q_{Gi} \leq Q_{Gi.\max},$$
$$i \in \{1, 2, \ldots, N_G\}. \tag{26}$$

where $Q_{Gi.min}$ and $Q_{Gi.max}$ are lower and upper limits of the reactive power output of the ith generator; Q_{Gi} is the actual reactive power output of the ith generator.

b: BUS VOLTAGE CONSTRAINT

The constraint of RPD is the same as that of APD, expressed as (20).

c: TRANSMISSION SECURITY CONSTRAINT

The constraint of RPD is the same as that of APD, expressed as (21).

d: LOAD FLOW EQUALITY CONSTRAINT

The constraint describes the nonlinear equalities of active and reactive power balance, which is expressed as (17) and (18).

e: TRANSFORMER CONSTRAINT

The tapping configuration of every transformer is limited as:

$$T_{a.\min} \leq T_a \leq T_{a.\max}, \quad a \in \{1, 2, \ldots, N_T\}. \tag{27}$$

where $T_{a.min}$ and $T_{a.max}$ are the lower and upper tapping limits of the ath transformer; T_a is the actual tapping of the ath transformer, and N_T is the number of transformers.

f: VAR SOURCE CONSTRAINT

The reactive power generated by every VAR source is limited in a practical range:

$$Q_{Cb.\min} \leq Q_{Cb} \leq Q_{Cb.\max}, \quad b \in \{1, 2, \ldots, N_C\}. \tag{28}$$

where $Q_{Cb.min}$ and $Q_{Cb.max}$ are the lower and upper reactive power output limits of the bth VAR source; Q_{Cb} is the actual reactive power output of the bth VAR source, and N_C is the number of VAR sources.

IV. COMPUTATION STUDIES

A. METRICS OF EVALUATION

When solving the multi-objective problems, it is difficult to obtain the true Pareto front. Therefore, there are several metrics proposed to evaluate the performances of the corresponding algorithm.

1) SPACING

The spacing metric [19], [20] is defined to measure how evenly the Pareto solutions are distributed along the obtained Pareto front and calculated as:

$$S = \sqrt{\frac{1}{n_f} \sum_{i=1}^{n_f} (d_i - d_{avg})^2}, \tag{29}$$

where d_i is the Euclidean distance between the ith solution and its nearest solution, and n_f is the number of solutions, and d_{avg} is the mean value of all d_i in the obtained Pareto front.

2) SPAN

The span metric [21] measures the maximum extent of each objective function to estimate the range to which the obtained Pareto front spreads out, calculated as:

$$SP = \sqrt{\sum_{i=1}^{M} (f_{i.\max}^* - f_{i.\min}^*)^2}. \tag{30}$$

where M is the number of the objective functions; $f_{i.max}*$ and $f_{i.min}*$ are the normalized maximum and minimum function values of the ith objective. For the cases with two objectives, the span metric is equal to the distance of the two outer solutions.

3) CONVERGENCE

The convergence metric [10] measures the extent of the obtained Pareto front's convergence to a known or true Pareto-optimal front. For each solution of the obtained Pareto front, the minimum value of the Euclidean distances of it from all the solutions of the known or true Pareto front is calculated. And the average value of those minimum distances is obtained as the convergence metric.

4) l_{max}/l_{min}

l_{max}/l_{min} [20] is defined as the ratio of the maximum Euclidean distance and the minimum Euclidean distance of adjacent solutions, which is used to measure the uniformity of the Pareto solution.

5) CONVERGENCE TIME

This metric refers to the total time needed for the objective values and other metrics achieving the requirements using the corresponding algorithm.

B. SETTING OF THE TEST SYSTEM

To test the performances of the proposed MO-MFO algorithm's application in multitasking electric power dispatch, the IEEE-118-bus and IEEE-30-bus systems [4] are chosen for the active and reactive power dispatch tasks, respectively. The IEEE-118-bus system consists of 186 branches and 54 generators. The IEEE-30-bus system consists of 41 branches and 6 generators and has 12 variables, including 6 generator voltages, 4 tapping ratios of the OLTC transformers connected in the branches 4-12, 6-9, 6-10, and 27-28 respectively, and 2 shunt capacitors installed at buses 10 and 24.

To compare different algorithms fairly, the population numbers of IEEE-118-bus and IEEE-30-bus systems are set to be 100 and 300 respectively and the maximum number of iterations is set to be 1000. The computation results of the proposed and other algorithms are based on 30 runs of iterations.

C. COMPUTATION RESULTS

In the previous setting, there are two multi-objective optimization tasks: the first one is the active power dispatch for the IEEE-118-bus system; and the second one is the reactive power dispatch for the IEEE-30-bus system.

1) TASK 1-ACTIVE POWER DISPATCH FOR THE IEEE-118-BUS SYSTEM

In the computations of task 1, the economic and environmental objectives are chosen as the optimization objectives, and the performance metrics of different algorithms after 30 runs of iterations are shown in Table 1. The proposed MO-MFO method is verified to be more advantageous as compared to the NSGA-II, MGSO, and MOEA/D algorithms

TABLE 1. Performance metrics of different algorithms of task 1.

Metrics	Algorithms	Best	Worst	Average	Variance
Spacing	NSGA-II	0.093461	0.291375	0.186027	**3.5419E-5**
	MGSO	0.110946	0.341046	0.187109	0.008641
	MOEA/D	0.078954	0.293110	0.157050	0.064736
	MO-MFO	**0.073981**	**0.276890**	**0.154421**	0.063697
Span	NSGA-II	0.991366	0.841553	0.935189	3.1072E-5
	MGSO	1.241689	0.849138	1.161152	2.4431E-6
	MOEA/D	1.696744	0.978471	1.432684	8.8589E-5
	MO-MFO	**1.755698**	**1.079517**	**1.466831**	**5.0362E-7**
Convergence	NSGA-II	0.029108	0.091567	0.055661	0.006152
	MGSO	0.017956	**0.089144**	0.054183	**0.001457**
	MOEA/D	0.016974	0.091667	0.055149	0.053179
	MO-MFO	**0.016606**	0.106417	**0.044342**	0.021830
l_{max}/l_{min}	NSGA-II	23.54207	211.6902	68.35971	1561.189
	MGSO	22.45910	**52.24871**	36.02057	**172.3400**
	MOEA/D	**9.112641**	53.57920	31.09650	231.3301
	MO-MFO	10.68151	57.26891	**29.45010**	256.7810

The best values are highlighted in bold.

TABLE 2. Comparisons of best solutions of task 1.

Task 1	Best Cost				Best Emission			
	NSGA-II	MGSO	MOEA/D	**MO-MFO**	NSGA-II	MGSO	MOEA/D	**MO-MFO**
P_{G1}	0.75494	0.67489	0.71703	0.75698	0.77765	0.74196	0.65787	0.69117
P_{G2}	0.71812	0.71504	0.62391	0.76722	0.79418	0.70828	0.83877	0.72574
P_{G3}	0.79977	0.47088	0.72078	0.67157	0.43394	0.87034	0.56071	0.74940
P_{G4}	0.75273	0.60024	0.83358	0.70111	0.65115	0.61475	0.70419	0.81953
P_{G5}	0.78230	0.36872	0.47811	0.85938	0.40965	0.96336	0.35649	0.66948
P_{G6}	1.34860	0.87533	0.72017	0.97457	1.13886	0.41487	0.73726	1.11659
P_{G7}	0.94474	0.75147	0.93600	0.83699	0.73673	0.88315	0.79363	0.97016
P_{G8}	0.73888	0.66675	0.77713	0.79654	0.61837	0.64231	0.80874	0.74973
P_{G9}	0.74108	0.74694	0.78735	0.94572	0.74284	0.74342	0.65078	0.72566
P_{G10}	0.70435	0.75390	0.88200	0.67992	0.64920	0.77633	0.56824	0.41837
P_{G11}	0.76313	0.34987	1.31146	0.78445	1.24344	0.77970	0.44680	0.70791
P_{G12}	0.23269	0.39160	0.73090	0.66714	0.77708	0.75834	0.57662	0.48125
P_{G13}	0.84789	0.34215	0.85835	0.75268	0.45080	0.35755	0.77014	0.76040
P_{G14}	0.85726	0.77200	0.78506	0.72016	0.87478	0.86034	0.93656	0.93555
P_{G15}	0.87118	0.81081	0.71410	0.92614	0.78684	0.73947	0.92936	0.99609
P_{G16}	0.96701	0.87893	0.88591	0.98102	0.80940	0.90866	0.94158	0.81091
P_{G17}	0.87420	0.95198	0.83095	0.88707	0.997/4	0.85088	0.92984	0.80963
P_{G18}	0.91610	0.90080	0.95353	0.92710	0.96120	0.91477	0.95964	0.91154
P_{G19}	0.93656	0.72710	0.89715	0.81423	0.83418	0.95329	0.86336	0.91146
P_{G20}	0.78435	1.03195	0.98643	0.85771	0.64222	1.35824	0.84462	0.94454
P_{G21}	1.34208	0.45620	0.79289	1.36188	0.76152	0.43910	0.78689	0.78242
P_{G22}	0.62813	1.31549	0.67021	0.90828	0.68875	1.33967	0.98868	0.44481
P_{G23}	0.87103	0.75070	0.70450	0.86982	0.89028	0.70274	0.87366	0.90285
P_{G24}	0.78646	0.89715	0.98712	0.86815	0.70143	0.97100	0.73531	0.80986
P_{G25}	1.45472	1.31187	1.06196	1.65420	1.10608	1.45062	1.24088	1.31979
P_{G26}	0.81714	0.93013	1.04789	0.81906	0.90051	1.00616	0.85978	0.95824
P_{G27}	0.73749	0.61167	0.86887	0.67708	0.81081	0.87460	0.88689	0.71433
P_{G28}	0.86454	1.09373	0.48234	0.77687	0.65978	1.04581	0.36780	0.63059
P_{G29}	1.32697	1.25257	0.95420	0.77460	0.97021	1.17749	0.79052	0.91716
P_{G30}	0.69558	0.11616	0.09511	0.66470	0.79735	0.85755	0.35726	0.27651
P_{G31}	0.61433	0.87100	0.13531	1.06196	0.43816	0.78094	0.77309	0.63795
P_{G32}	0.40143	0.23555	0.30051	0.65824	0.70285	0.98234	0.45875	0.71999
P_{G33}	0.26454	0.55472	0.70143	0.15766	0.61979	0.75875	0.75248	0.53004
P_{G34}	0.86815	0.97687	0.55062	0.89879	0.74088	0.97687	0.74581	0.75083
P_{G35}	0.75834	0.67335	0.75874	0.87510	0.75083	0.96815	0.75835	0.88125
P_{G36}	0.81154	0.57662	0.75062	0.79052	0.75978	0.77309	0.73418	0.73749
P_{G37}	1.95257	1.71167	0.81167	0.68201	0.43555	1.37118	0.97510	0.98162
P_{G38}	0.76470	0.83004	0.75766	0.83269	0.87651	0.79289	0.76780	0.90051
P_{G39}	0.48646	0.41714	0.45420	0.49373	0.46454	0.42697	0.44088	0.44581
P_{G40}	0.81999	1.01979	0.71716	0.99373	0.94722	0.85257	0.91714	0.96196
P_{G41}	0.77118	0.88712	0.76034	0.73090	0.99715	0.72697	0.73656	0.87749
P_{G42}	0.80051	0.45248	0.75726	0.66470	0.77478	0.67021	0.61716	0.59052
P_{G43}	0.83004	0.80285	0.79735	0.81906	0.65080	0.75766	0.73795	0.88712
P_{G44}	0.76887	0.66034	060986	0.65874	0.75329	0.61154	0.71187	0.73059
P_{G45}	0.94789	0.93013	1.08094	0.78875	0.92710	1.09160	0.81038	0.90274
P_{G46}	0.35080	0.41038	0.47335	0.41146	0.78187	0.39879	0.65248	0.59160
P_{G47}	0.74215	0.51506	0.78162	0.67366	0.45887	0.40608	0.98201	0.71616
P_{G48}	0.65268	0.68201	0.77014	0.74478	0.77200	0.74511	0.91146	0.48234
P_{G49}	0.49558	0.60274	0.90608	0.82016	0.61999	0.89289	0.57749	0.77366
P_{G50}	0.34215	0.73714	0.61506	0.75875	0.87014	0.57651	0.64511	0.45268
P_{G51}	0.48162	0.80986	0.78689	0.76040	0.73816	0.76040	0.76714	0.47460
P_{G52}	0.85834	0.45835	0.59735	0.43013	0.78094	0.61433	0.31906	0.58875
P_{G53}	0.57200	0.83059	0.92016	0.77662	0.51154	0.76780	0.63090	0.25755
P_{G54}	0.83269	0.77309	0.87708	0.68125	0.73418	0.71081	0.97510	0.95329
Cost	63734.2	63619.8	63566.1	**63346.2**	73713.0	73833.4	73234.8	75176.3
Emission	2.86489	2.87230	2.87745	2.89499	2.62146	2.62956	2.62374	**2.60813**

The best values are highlighted in bold.

when applied in electric power dispatches. From Table 1, the spacing values and the average l_{max}/l_{min} of the MO-MFO
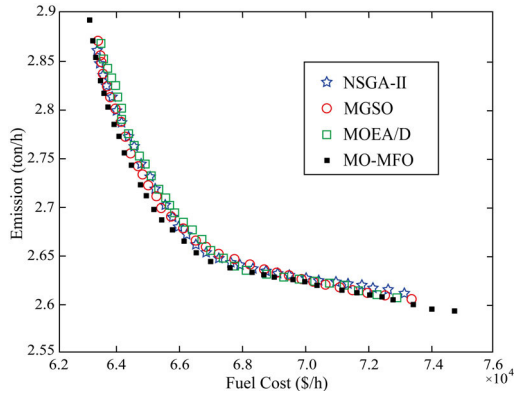
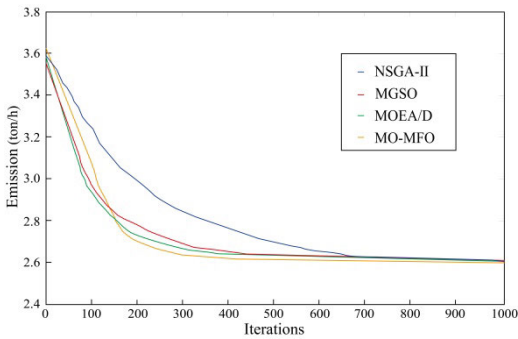**FIGURE 4.** Comparison of the Pareto fronts of task 1.

FIGURE 5. Comparison of convergences of emission objective of task 1.

algorithm are the lowest than the others, meaning that its Pareto solutions are distributed the most evenly. The span values of the MO-MFO algorithm are the largest among those algorithms, indicating its largest search ranges. Table 2 presents the best solutions of cost and emission calculated from the extreme points of the resulting Pareto fronts of the algorithms. As compared to other algorithms, the MO-MFO has lower cost and emission objective values of the best solutions. Besides, the best Pareto fronts obtained from the algorithms are plotted in Fig. 4. As compared to the other algorithms, the Pareto front obtained from the MO-MFO algorithm is closer to the left bottom point and with two better outer solutions. Moreover, the convergences of the emission objectives obtained from the different algorithms are given in Fig. 5, which shows that the MO-MFO has better convergence time.

2) TASK 2–REACTIVE POWER DISPATCH FOR THE IEEE-30-BUS SYSTEM

In the computations of task 2, the transmission loss and the voltage deviation are selected as the optimization objectives, and the performance metrics of different algorithms after 30 runs of iterations are shown in Table 3, from which it can be observed that the average values of spacing, span, convergence, and l_{max}/l_{min} metrics of the MO-MFO algorithm are the best. Table 4 presents the best solutions of transmission loss and voltage deviation calculated from the extreme points of the resulting Pareto fronts of the algorithms. As compared to other algorithms, the MO-MFO has lower

TABLE 3. Performance metrics of different algorithms of task 2.

Metrics	Algorithms	Best	Worst	Average	Variance
Spacing	NSGA-II	0.054894	**0.215897**	0.164860	0.001671
	MGSO	**0.041143**	0.238460	0.166941	0.009348
	MOEA/D	0.045681	0.247898	0.158871	**0.001355**
	MO-MFO	0.077689	0.226559	**0.158102**	0.002147
Span	NSGA-II	0.995784	0.965800	0.986655	5.3293E-4
	MGSO	1.195864	0.915602	1.011150	6. 236E-4
	MOEA/D	1.246868	1.020369	1.163159	0.009342
	MO-MFO	**1.365973**	**1.126661**	**1.267674**	**5.7654E-5**
Convergence	NSGA-II	0.012332	0.172236	0.106239	**0.002317**
	MGSO	0.010164	**0.154269**	0.128675	0.058144
	MOEA/D	0.009412	0.188367	0.087992	0.021170
	MO-MFO	**0.009139**	0.170440	**0.083361**	0.057162
l_{max}/l_{min}	NSGA-II	11.95160	57.2198	37.14861	1147.035
	MGSO	16.35971	67.69448	33.19799	219.0534
	MOEA/D	7.593311	42.95944	20.54897	163.5920
	MO-MFO	**7.259866**	**41.00569**	**19.57940**	**130.25527**

The best values are highlighted in bold.

TABLE 4. Comparisons of best solutions of task 2.

Task 2	Best P_{loss}				Best V_D			
	NSGA-II	MGSO	MOEA/D	**MO-MFO**	NSGA-II	MGSO	MOEA/D	**MO-MFO**
V_{G1}	1.0500	1.0500	1.0500	1.0500	1.0429	1.0094	1.0461	1.0354
V_{G2}	1.0443	1.0445	1.0478	1.0442	1.0368	1.0250	1.0070	1.0184
V_{G3}	1.0226	1.0227	1.0229	1.0223	1.0087	1.0162	1.0201	1.0205
V_{G4}	1.0247	1.0265	1.0257	1.0262	1.0057	1.0068	1.0072	1.0056
V_{G5}	1.0950	1.0675	1.0714	1.0676	1.0493	1.0615	1.0670	1.0278
V_{G6}	1.0772	1.0757	1.0788	1.0884	1.0498	1.0461	1.0136	1.0338
T_{6-9}	1.050	1.000	1.070	1.070	1.050	1.050	1.050	1.050
T_{6-10}	0.900	0.966	0.900	0.975	0.900	0.900	0.900	0.900
T_{4-12}	1.000	1.000	1.000	1.000	1.000	1.000	1.000	1.000
T_{27-28}	1.050	1.050	1.050	1.050	1.050	1.050	1.050	1.050
Q_{C10}	0.19	0.19	0.19	0.19	0.19	0.19	0.19	0.19
Q_{C24}	0.04	0.04	0.04	0.04	0.04	0.04	0.04	0.04
P_{loss}	0.0514	0.0512	0.0515	**0.0511**	0.0579	0.0574	0.0571	0.0573
V_D	0.5929	0.6056	0.5917	0.6351	0.1789	0.1667	0.1761	**0.1660**

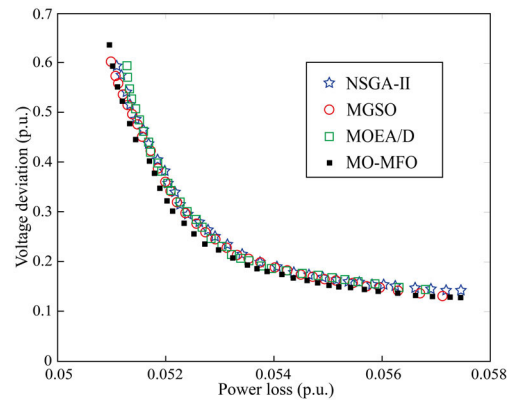The best values are highlighted in bold.

FIGURE 6. Comparison of the Pareto fronts of task 2.

transmission loss and voltage deviation objective values of the best solutions. From Fig. 6, the best Pareto front of the MO-MFO algorithm is closer to the left bottom point and with one better outer solution as compared to the other three algorithms. Fig. 7 shows the convergence processes of the transmission loss objective of different algorithms, and the MO-MFO algorithm exhibits fewer iterations.

3) MULTITASKING PERFORMANCE

With regards to the NSGA-II, MGSO, and MOEA/D algorithms, task 1 and task 2 are solved in series, while the MO-MFO algorithm solves the two tasks simultaneously.
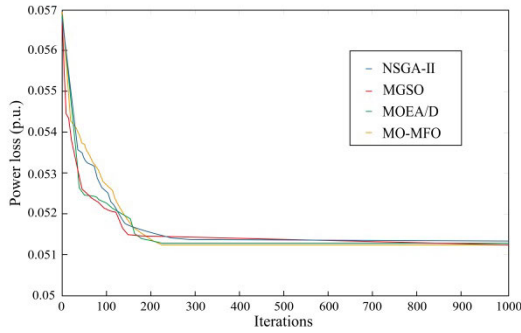
FIGURE 7. Comparison of convergences of transmission loss objective of task 2.

TABLE 5. Comparisons of convergence times of two tasks.

Algorithms		NSGA-II	MGSO	MOEA/D	MO-MFO
Run time (s)	Task 1	11.104	11.052	12.649	11.148
	Task 2	1.566	1.506	1.607	
	Total	12.670	12.558	14.256	**11.148**

The best values are highlighted in bold.

Their run times are presented in Table 5. It can be observed that the total run time of the two tasks of the MO-MFO algorithm is the shortest with at least 1.41s advantage as compared to the other algorithms. Besides, the aforementioned computation results, the overall performance metrics and solution qualities of the MO-MFO algorithm applied in the multitasking electric power dispatch problem are the best among the four algorithms.

V. CONCLUSION

In this paper, a multitasking electric power dispatch approach based on the MO-MFO algorithm is proposed to apply in complex electric power dispatch problems, specifically, the active and reactive power dispatches. As compared to the existing evolutionary techniques for electric power dispatch, including NSGA-II, MGSO, and MOEA/D methods, the proposed approach performs much better in terms of the evaluation metrics and solution qualities, as well as the computation efficiency. Moreover, the approach exhibits the great potential to be developed as a cloud-computing solver or platform for future large-scale smart grid applications involving different market entities because of its implicit parallel computation mechanism.

REFERENCES

[1] M. A. Abido, "Multiobjective evolutionary algorithms for electric power dispatch problem," *IEEE Trans. Evol. Comput.*, vol. 10, no. 3, pp. 315–329, Jun. 2006.

[2] T. F. Robert, A. H. King, C. S. Rughooputh, and K. Deb, "Evolutionary multi-objective environmental/economic dispatch: Stochastic versus deterministic approaches," KanGAL, Kanpur, India, Tech. Rep. 2004019, 2004, pp. 1–15.

[3] M. Abido and J. Bakhashwain, "Optimal VAR dispatch using a multiobjective evolutionary algorithm," *Int. J. Electr. Power Energy Syst.*, vol. 27, no. 1, pp. 13–20, Jan. 2005.

[4] B. Zhou, K. W. Chan, T. Yu, and C. Y. Chung, "Equilibrium-inspired multiple group search optimization with synergistic learning for multiobjective electric power dispatch," *IEEE Trans. Power Syst.*, vol. 28, no. 4, pp. 3534–3545, Nov. 2013.

[5] B. Zhou, K. W. Chan, T. Yu, H. Wei, and J. Tang, "Strength Pareto multigroup search optimizer for multiobjective optimal reactive power dispatch," *IEEE Trans. Ind. Informat.*, vol. 10, no. 2, pp. 1012–1022, May 2014.

[6] A. Gupta, Y.-S. Ong, and L. Feng, "Multifactorial evolution: Toward evolutionary multitasking," *IEEE Trans. Evol. Comput.*, vol. 20, no. 3, pp. 343–357, Jun. 2016.

[7] A. Gupta, Y.-S. Ong, L. Feng, and K. C. Tan, "Multiobjective multifactorial optimization in evolutionary multitasking," *IEEE Trans. Cybern.*, vol. 47, no. 7, pp. 1652–1665, Jul. 2017.

[8] Y.-S. Ong and A. Gupta, "Evolutionary multitasking: A computer science view of cognitive multitasking," *Cognit. Comput.*, vol. 8, no. 2, pp. 125–142, Apr. 2016.

[9] L. Feng, Y.-S. Ong, M.-H. Lim, and I. W. Tsang, "Memetic search with interdomain learning: A realization between CVRP and CARP," *IEEE Trans. Evol. Comput.*, vol. 19, no. 5, pp. 644–658, Oct. 2015.

[10] K. Deb, A. Pratap, S. Agarwal, and T. Meyarivan, "A fast and elitist multiobjective genetic algorithm: NSGA-2," *IEEE Trans. Evol. Comput.*, vol. 6, no. 2, pp. 182–197, Aug. 2002.

[11] K. Deb, "An efficient constraint handling method for genetic algorithms," *Comput. Methods Appl. Mech. Eng.*, vol. 186, nos. 2–4, pp. 311–338, Jun. 2000.

[12] L. L. Cavalli-Sforza and M. W. Feldman, "Cultural vs biological inheritance: Phenotypic transmission from parents to children (a theory of the effect of parental phenotypes on children's phenotypes)," *Amer. J. Hum. Genet.*, vol. 25, pp. 618–637, 1973.

[13] D. Xu, Q. Wu, B. Zhou, C. Li, L. Bai, and S. Huang, "Distributed multi-energy operation of coupled electricity, heating and natural gas networks," *IEEE Trans. Sustain. Energy*, early access, Dec. 23, 2020, doi: 10.1109/TSTE.2019.2961432.

[14] J.-B. Park, K.-S. Lee, J.-R. Shin, and K. Y. Lee, "A particle swarm optimization for economic dispatch with nonsmooth cost functions," *IEEE Trans. Power Syst.*, vol. 20, no. 1, pp. 34–42, Feb. 2005.

[15] D. B. Das and C. Patvardhan, "New multi-objective stochastic search technique for economic load dispatch," *IEEE Proc.-Generat. Transmiss. Distrib.*, vol. 145, no. 6, pp. 747–752, Nov. 1998.

[16] K. Lee, Y. Park, and J. Ortiz, "A united approach to optimal real and reactive power dispatch," *IEEE Trans. Power App. Syst.*, vol. PAS-104, no. 5, pp. 1147–1153, May 1985.

[17] F. N. Lee and A. M. Breipohl, "Reserve constrained economic dispatch with prohibited operating zones," *IEEE Trans. Power Syst.*, vol. 8, no. 1, pp. 246–254, Feb. 1993.

[18] P. Kessel and H. Glavitsch, "Estimating the voltage stability of a power system," *IEEE Trans. Power Del.*, vol. 1, no. 3, pp. 346–354, Jul. 1986.

[19] K. Deb, *Multi-Objective Optimization Using Evolutionary Algorithms*. Chichester, U.K.: Wiley, 2001.

[20] Q. Li, M. Liu, and H. Liu, "Piecewise normalized normal constraint method applied to minimization of voltage deviation and active power loss in an AC–DC hybrid power system," *IEEE Trans. Power Syst.*, vol. 30, no. 3, pp. 1243–1251, May 2015.

[21] E. Zitzler, K. Deb, and L. Thiele, "Comparison of multiobjective evolutionary algorithms: Empirical results," *Evol. Comput.*, vol. 8, no. 2, pp. 173–195, Jun. 2000.

JUNWEI LIU received the B.Eng. degree in water conservancy and hydropower engineering from the Huazhong University of Science and Technology, China, in 2012, and the Ph.D. degree from the Department of Electrical Engineering, The Hong Kong Polytechnic University, Hong Kong, in 2018.

He is currently a Postdoctoral Fellow with Shenzhen University, Shenzhen, China. His research interests include wireless power transfer, power electronics, and optimization algorithms in power systems.

PEILING LI received the B.Eng. degree in transportation engineering from Wuyi University, Jiangmen, China, in 2015, and the M.Eng. degree in transportation engineering from Shenzhen University, Shenzhen, China, in 2020.

Her research interests include electric vehicle charging and power system state estimation.

GUIBIN WANG (Member, IEEE) received the B.E. degree in electrical engineering from Shandong University, Jinan, China, in 2009, and the Ph.D. degree from Zhejiang University, Hangzhou, China, in 2014.

From 2011 to 2014, he was a Research Assistant with the Department of Electrical Engineering, The Hong Kong Polytechnic University, Hong Kong. He is currently an Associate Research Professor with Shenzhen University, Shenzhen, China. His main research interests include electric vehicles and renewable energy.

YONGXING ZHA received the B.S. degree in physics and electronics from Henan University, Kaifeng, China, in 2017, and the M.S. degree from the College of Mechatronics and Control Engineering, Shenzhen University, Shenzhen, China, in 2020.

His major research interests include power system control, multi-objective optimization, and integrated energy system scheduling.

JIANCHUN PENG (Senior Member, IEEE) received the B.S. and M.S. degrees in electrical engineering from Chongqing University, Chongqing, China, in 1986 and 1989, respectively, and the Ph.D. degree in electrical engineering from Hunan University, Hunan, China, in 1998.

From November 2002 to November 2003, he was a Visiting Professor with Arizona State University, Tempe, AZ, USA. From May 2006 to August 2006, he was with Brunel University, London, U.K. He is currently a Professor with the College of Mechatronics and Control Engineering, Shenzhen University, Shenzhen, China. His current research interests include electricity markets, and power system optimal operation and control.

GANG XU received the B.S. degree in control engineering from Beihang University, Beijing, China, in 1982, and the Ph.D. degree in engine-control engineering from the Nanjing University of Aeronautics and Astronautics, Nanjing, China, in 1995.

From 1987 to 1989, he was a Visiting Research Fellow with Louisiana State University, Baton Rouge, LA, USA. From 1996 to 1997, he was a Postdoctoral Researcher with Sussex University, Brighton, U.K. From 1998 to 2017, he was a Professor with the College of Mechatronics and Control Engineering, Shenzhen University, Shenzhen, China. Since 2017, he has been with the College of Urban Transportation and Logistics, Shenzhen Technology University, Shenzhen. His research interests include aero-engines, electric vehicles, and traffic engineering.

● ● ●